2025 IMEKO TC26 International Conference on
Metrology for Archaeology and Cultural Heritage
Bergamo, Italy, October 15-17, 2025

Dust Detector for Museum Environment Based on Raspberry Pi

Mariagrazia Leccisi[1], Giuseppe Schirripa Spagnolo[2], Fabio Leccese[1]

[1] *Dipartimento di Scienze, Università degli Studi Roma Tre, via della Vasca Navale n.84, 00146 Rome, Italy, mariagrazia.leccisi@uniroma3.it, fabio.leccese@uniroma3.it*
[2] *Dipartimento di Matematica e Fisica, Università degli Studi "Roma Tre", via della Vasca Navale n.84, 00146 Rome, Italy, giuseppe.schirripaspagnolo@uniroma3.it*

***Abstract* – Using a Raspberry Pi, we have created a low-cost, easily implementable, scalable and highly integrable system, suitable for real and extensive applications for dust detection within museum environments. In order to catch the dust, the Raspberry Pi uses a high-definition camera module on which dust settles. After the acquisition of the image, the platform is able to recognize and to cluster the single particles using a custom-developed image recognition software that runs on the Raspberry. The first analysis and consequent results are promising.**

I. INTRODUCTION

One of the main issues affecting museum environments is the progressive deterioration caused by environmental factors such as light exposure, relative humidity, thermal fluctuations, biological agents, and atmospheric pollutants. These pollutants may originate from both external and internal sources, in the form of airborne particulate matter (dust) and volatile substances, including volatile organic compounds (VOCs), alkaline particles from construction materials, and emissions from conservation or exhibition materials. These contaminants typically enter museum interiors through natural or mechanical ventilation systems but may also be introduced inadvertently by visitors through their clothing, hair, skin, or personal items [1]. The transported particulate matter comprises a wide range of materials, such as textile fibres, soil fragments, hair, vegetal or animal debris, spores, and insects, with particle sizes ranging approximately from one to three hundreds µm [2]. Depending on their mass, larger particles tend to settle on horizontal surfaces by gravity, while finer particles adhere to substrates via electrostatic forces.

The impact of such particles on museum objects has been widely documented. For instance, combustion residues such as soot can form dark deposits that alter the visual appearance of surfaces; the presence of dust also facilitates condensation of water vapour, contributing to hygroscopic deterioration and promoting microbial growth. This microbial activity may result in the formation of biofilms capable of trapping additional airborne matter, increasing the potential for damage [3-6]. Moreover, the presence of dust may lead to micro abrasions during cleaning operations, further endangering sensitive materials [7]. Gaseous pollutants also pose a significant risk to exhibited materials. Documented effects include carbonate dissolution in calcareous substrates, discoloration and stiffening of leather, brittleness of fabrics, efflorescence in fossils, and corrosion of metals. For these reasons, it is essential to implement efficient, continuous, and non-invasive monitoring systems capable of supporting preventive conservation strategies through the identification, quantification, and spatial mapping of airborne pollutants within museum spaces.

II. CURRENT TECHNOLOGIES

Current technologies employed for air quality assessment in museum environments focus on the identification of pollutants introduced through mechanical or natural ventilation systems or carried in by visitors. This assessment is typically conducted through passive sampling methods, followed by physicochemical analyses [8-10].

To monitor the presence of textile fibres, dust, and particulate matter, adhesive sampling surfaces (made of materials such as Teflon, vinyl, or other inert polymers) are strategically positioned within the environment and left in place for a predetermined exposure period.

The collected samples are subsequently analysed using optical microscopy, scanning electron microscopy (SEM), or ion chromatography, to determine the chemical composition and possible sources of contamination [10-14].

In addition to passive sampling, optical particle detection instruments are also employed to quantify airborne particulate concentrations. Nephelometers, for example, utilize a laser-illuminated chamber in which particles scatter light; the scattered light is detected by photodetectors, generating signals that correlate with particle size and concentration [15,16].

Aethalometers are designed to specifically target black carbon: particles are retained on quartz fibre filters, and the reduction in transmitted light intensity through the filter is inversely proportional to the amount of light-absorbing

carbonaceous material deposited [17].

For continuous airborne pollutant monitoring, Wireless Sensor Networks (WSNs) represent an advanced technological solution. These systems integrate nodes equipped with sensors, microprocessors, memory units, transceivers, and batteries, enabling real-time acquisition and transmission of environmental data [18-20]. However, their practical use is limited by constraints related to memory capacity, battery life, and communication range.

The accuracy and effectiveness of such monitoring strategies increase proportionally with the density of collected samples, which allows for meaningful correlations between contaminant presence or concentration and several influencing factors, such as visitor flow and occupancy levels, ventilation duration and frequency, proximity to architectural openings such as doors and windows, which act as pollutant entry points.

Despite their precision, these systems often rely on expensive instrumentation and complex physicochemical analyses, making them less accessible and harder to scale.

As a simplified and cost-effective alternative, image-based analysis has proven to be a valid method for the visual characterization of airborne particulate matter and fibres, by extracting morphological parameters such as shape, size, and orientation [21-24].

For example, circular elements typically indicate the presence of solid particulate matter of mineral or organic origin, while filamentous structures are usually associated with textile fibres, whether natural or synthetic.

Fibres can also be distinguished based on length and diameter; for example, clothing-derived fibres are generally thinner than those from carpets (threshold of approximately 30 μm), while longer fibres, often originating from human hair or animal fur, can be distinguished by their diameter, with animal hairs often measuring less than half the diameter of human hair [25,26].

The proposed system differs from traditional monitoring tools, which are typically expensive and complex, because it uses low-cost hardware and automated image analysis techniques to recognize not only the quantity but also the morphology of particles. Maintenance is also simple and cost-effective. This combination enables portable, replicable monitoring, applicable in museum settings.

III. SYSTEM ARCHITECTURE

The proposed system is designed to acquire, process, and visually classify dust and fibre particles that settle on an inclined surface, to analyse their morphology using computer vision techniques. The system architecture is based on low-cost hardware components, combined with open-source software tools executed on a Raspberry Pi platform.

The overall setup is compact, self-contained, and designed for autonomous operation, requiring minimal human intervention. Its reduced footprint and automated acquisition pipeline make it particularly well-suited for continuous monitoring in space-constrained or sensitive environments, such as museums and archival storage areas. Fig.1 shows the architecture of the system.

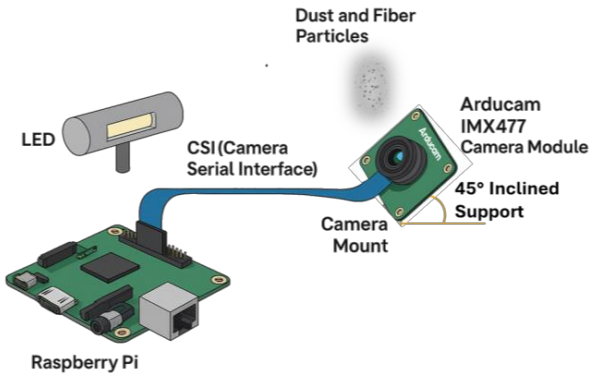

Fig. 1. The architecture of the system.

A. Hardware

The Raspberry Pi 4, running the lightweight Raspberry Pi OS Lite operating system and a Python environment for executing acquisition and processing scripts, serves as the central unit for data collection, control, and computation. The optical subsystem employs an Arducam camera module based on the Sony IMX477 sensor, a 12.3 megapixel back-illuminated CMOS sensor with a native resolution of 4056 × 3040 pixels. The sensor features a pixel size of 1.55 μm × 1.55 μm, offering a balance between sensitivity and resolution, and is suitable for imaging particulate matter and fibers ranging from 5 μm to several hundred μm, depending on the lens configuration. The camera interfaces with the Raspberry Pi via MIPI CSI-2 (4-lane) connection and supports interchangeable C/CS-mount lenses, enabling fine optical adjustment based on the required field of view and magnification. The camera is mounted on a mechanical support inclined at 45°, a configuration designed to maximize particle deposition within the field of view through gravitational settling. This geometrical arrangement enhances the ability to capture particles in situ without active collection mechanisms. Lighting was provided by a compact USB LED lamp (5500 – 6000 K, CRI ⩾ 90), with small dimensions (< 15 cm) and a flexible neck for tangential positioning on the deposition surface (Fig.1), which makes the variability of ambient light irrelevant. This configuration ensures uniform and stable lighting without cluttering the operating space and can be easily powered by the Raspberry Pi.

This lighting geometry enhances the visual separability between the particulate elements and the background, facilitating subsequent image segmentation and classification.

For the lifetime of the system, having been manufactured with COTS (Components off the Shelf)

components, the device does not require any special maintenance [27,28]. Cleaning of the lens, the only element requiring maintenance, can be carried out at regular intervals in accordance with the conservation experts who manage the monitored area.

B. Operating flow

The operational flow involves the periodic acquisition of images, with optional automated scheduling, using libcamera for capture and OpenCV-Python for processing.

The first stage of pre-processing aims to optimize the quality and visual consistency of the acquired images by eliminating optical, environmental, or digital noise that may interfere with proper segmentation and classification. This step is particularly crucial in applications where the integrity of shape and proportion of the observed particles is critical.

Initially, the RGB image captured by the camera is converted into grayscale via a weighted combination of the color channels, to remove chromatic components irrelevant to analysis and standardize images captured under varying lighting conditions.

Subsequently, the contrast between particles and background is enhanced using pixel intensity redistribution techniques, resulting in an image where local intensity variations (e.g., between dust and background) are amplified.

Due to the 45° inclination of the camera and the non-uniform lighting, images often exhibit background intensity gradients that may compromise segmentation. To correct this artifact, a background estimation is performed by correlating the equalized image with a Gaussian low-pass filter with standard deviation σ, followed by subtraction of the estimated background from the equalized image, according to the formula

$$I_{corr}(x,y) = I_{eq}(x,y) - G_\sigma * I_{eq}(x,y)$$

This process emphasizes only high-frequency components (i.e., the particles), effectively removing background variations.

In this work, the standard deviation σ of the Gaussian low-pass filter was not fixed, but adjusted within the range 10–20 pixels, depending on image resolution and lighting conditions. Lower σ values were sufficient when illumination was uniform, whereas higher σ values were required in the presence of stronger background gradients. This adaptive choice ensured effective suppression of large-scale background variations while preserving particle boundaries across different experimental settings.

Since the aim is to optimally separate the background pixels from those of the particles, in accordance with the literature, it was decided to use Otsu's automatic threshold.

To separate the particles from the background, a global automatic thresholding method is used, calculated with Otsu's algorithm, which determines the threshold that minimizes intra-class variance between foreground and background. The resulting binary image contains white pixels representing the background and black pixels corresponding to particles.

To further eliminate residual noise, a median filter is applied, which is highly effective at preserving particle boundaries. Compared to an average filter (blur), the median filter better preserves contours, which is essential for distinguishing the morphology of fibers from circular granules.

C. Image Segmentation and Data Structuring

Following pre-processing, which yields an optimized binary matrix, the next step is to structure the data for classification. To this end, the image is segmented into nonoverlapping square blocks, forming a grid. This block-based segmentation, reduces computational complexity, allows independent analysis of each block, enhances local stability of conditions and ensures spatial invariance of particle positioning.

The block size is a critical design parameter: smaller blocks (<30 px) offer higher spatial resolution but may lack sufficient information for reliable classification; larger blocks (>80 px) risk containing mixed particle types, reducing classification accuracy.

D. Classification

After segmentation, the system proceeds with classification, which represents its core decision-making component. The process employs a non-parametric supervised algorithm, specifically the k-Nearest Neighbours (k-NN) method.

For each block, a feature vector is computed, containing morphological and statistical descriptors selected for their ability to discriminate between circular and filamentous shapes. These features include the total number of black pixels (indicating deposit density), the number of connected components, mean component area, mean area-to-perimeter ratio, mean length, width and orientation

All feature values are normalized between 0 and 1 to avoid scale-related bias.

The k-NN classifier assigns a class to the test block by comparing it with the k most similar blocks in the labelled dataset, based on a distance metric. Several distance metrics were tested in this study as the Euclidean distance, Manhattan distance, Chebyshev distance and Hamming distance.

Among these, due to the binary and discretized nature of the extracted features, Hamming distance yielded the best performance. Unlike continuous metrics such as Euclidean or Manhattan distance, Hamming distance more effectively captures differences in categorical representations, leading to improved discrimination between circular and filamentous shapes.

IV. EXPERIMENTAL SETUP

The experimental phase aimed to evaluate the effectiveness of the proposed approach in the automatic

classification of image blocks containing dust or fibre particles. The analyses were conducted by systematically varying three key parameters of the classification system:

- the block size used for image segmentation (ranging from 30 to 80 pixels),
- the value of *k* in the k-Nearest Neighbors (k-NN) classifier (1, 3, 5, 7, 9),
- the type of distance metric adopted (Euclidean, Manhattan, Chebyshev, Hamming).

Following the preprocessing stage, images with a resolution of **1920×1080 px** were segmented into non-overlapping square blocks of **50 px**, which was identified as an optimal size for balancing spatial detail and classification accuracy. This configuration yielded approximately **777 blocks per frame** (38×2038 \times 2038×20), a number that falls within the desirable range (500–1500 blocks per image) for ensuring sufficient statistical robustness while keeping computational demands manageable on a Raspberry Pi platform. Smaller blocks (<30 px) would generate an excessive number of low-information segments, while larger blocks (>80 px) would significantly reduce the total number of blocks (e.g., fewer than 300 per frame), with a higher probability of mixing particle types within the same block.

V. EXPERIMENTAL RESULTS

In terms of classification accuracy, the best performance was achieved using the Hamming distance, with k=1 and a block size of 50 pixels. Specifically, results showed that accuracy increases with block size up to a maximum at 50 pixels, after which it decreases again. This trend suggests that smaller blocks may not contain sufficient discriminative information, whereas larger blocks may suffer from class mixing effects, leading to reduced classification performance.

Furthermore, values of k over or equal 5 tend to produce overgeneralization, diminishing the classifier's ability to distinguish fine morphological differences between classes.

From a qualitative standpoint, blocks containing thin and elongated elements, typically corresponding to fibrous particles, were recognized with high precision primarily due to their distinct orientation and length-to-width ratio.

Likewise, blocks containing circular particles, although variable in size, presented compact patterns that were easily distinguishable, while empty blocks (i.e., containing no particles) were also correctly classified in most cases.

A very limited number of false positives were observed, mainly attributable to residual noise or optical artefacts.

CONCLUSIONS

The developed system has proven to be functional, effective, and reliable for the automatic identification and classification of dust and fibre particles deposited in controlled environments. Specifically, the approach based on image analysis and morphological classification enabled the achievement of high accuracy levels (>90%) with minimal computational processing and without the need for expensive or invasive analytical instrumentation.

From a hardware perspective, the use of a compact platform such as the Raspberry Pi, combined with a high-definition camera module, allowed for the development of a low-cost, easily implementable, scalable, and highly integrable system suitable for real-world applications.

The simple mechanical setup, including a camera mounted at a 45° angle to promote the natural gravitational deposition of airborne particles, makes the system particularly suitable for use in sensitive contexts such as museums and galleries, where dust acts as a degradation agent for artworks and artefacts, exhibition spaces or archives, where continuous monitoring of environmental contamination is crucial and must occur without interfering with preserved objects, are crucial.

The absence of moving parts and the autonomous operation of the system further support its suitability for continuous and discreet monitoring, which can be integrated into distributed sensor networks. Looking ahead, the system can be further enhanced through environmental sensors (e.g., temperature, humidity, air flow), deep learning algorithms for advanced particle recognition (for example other more modern algorithms, such as CNNs (Convolutional Neural Network) instead of the current k-NN), and real-time dashboards for visualizing deposition data and trends.

REFERENCES

[1] A.A. Abdel Hameed, S. El-Gendy, Y. Saeed, "Characterization and decontamination of deposited dust: A management regime at a museum." Aerobiologia, 2024, pp.217-232

[2] H. Lloyd, C. M. Grossi, P. Brimblecombe, "Low-technology dust monitoring for historic collections", Journal of the Institute of Conservation, 2011, 34.1: 104-114.

[3] V. Agarwal, V. Abd El, S. G. Danelli, E. Gatta, D. Massabò, F. Mazzei, B. Meier, P. Prati, V. Vernocchi, J.Wang, "Influence of CO_2 and Dust on the Survival of Non-Resistant and Multi-Resistant Airborne *E.coli* Strains", Antibiotics, 2024, *13*(6), 558, https://doi.org/10.3390/antibiotics13060558

[4] Tiziana N. Beltrame, "A Matter of Dust, Powdery Fragments, and Insects. Object Temporalities Grounded in Social and Material Museum Life". Centaurus, 2023, 65.2: 365-385.

[5] O. Abdel-Kareem, S. Samaha, K. Elnagar, D. Essa, H. Nasr, "Monitoring the environmental conditions and their role in deterioration of textiles collection in museum of faculty of archeology, cairo university", Egypt. , 2022, 71-82. 10.5281/zenodo.6640272.

[6] H. Halbouni, et al. "Indoor Environment & Soiling Defects from Airborne Particulates towards Artefacts, Tourists, Visitors and Staff at the National

Museum Kuala Lumpur", 3rd International Conference on Creative Multimedia 2023 (ICCM 2023). Atlantis Press, 2023. p. 272-290.

[7] H. Wilson, S. Vansnick, "The effectiveness of dust mitigation and cleaning strategies at The National Archives", UK. Journal of Cultural Heritage, 2017, 24: 100-107.

[8] B.Terry, K. M. Shakya, "Monitoring gaseous pollutants using passive sampling in the Philadelphia region". Journal of the Air & Waste Management Association, 2023, 74(1), 52–69. https://doi.org/10.1080/10962247.2023.2279733

[9] I. Kraševec, E. Menart, M. Strlič, et al. "Validation of passive samplers for monitoring of acetic and formic acid in museum environments". Herit Sci 9, 19, 2021. https://doi.org/10.1186/s40494-021-00495-3

[10] C. García-Florentino, M. Maguregui, J. A. Carrero, H. Morillas, G. Arana, J. M. Madariaga," Development of a cost effettive passive sampler to quantify the particulate matter depositions on building materials over time", Journal of Cleaner Production, Volume 268, 2020, 122134, ISSN 0959-6526, https://doi.org/10.1016/j.jclepro.2020.122134.

[11] S. Brizzi, B. Łydżba-Kopczyńska, C. Riminesi, B. Salvadori, T. Sawoszczuk, M. Strojecki, O. Syta, D. Thickett, J. Torres-Elguera, A. Towarek, M. Sawicki, B. Wagner, "Surveying analytical techniques for a comprehensive analysis of airborne particulate samples in museum environments", TrAC Trends in Analytical Chemistry, Volume 176, 2024, 117766, ISSN 0165-9936, https://doi.org/10.1016/j.trac.2024.117766.

[12] R. Morello, C. De Capua, A.M. Gennaro, L. Fabbiano, "Characterization of material alterations in archaeological discoveries using thermography and emissivity changes" 2024 Acta IMEKO, 13 (4), DOI: 10.21014/actaimeko.v13i4.1862

[13] D. Duran-Romero, et al. "Assessment of Dust Deposition through Image Analysis in Complex and Remote Exhibition Sites: Study in the Cloister of the Santa María de El Paular Monastery in the Sierra de Guadarrama, Spain". Sustainability, 2024, 16.10: 4257

[14] S. Molaie, P. Lino, "Review of the newly developed, mobile optical sensors for real-time measurement of the atmospheric particulate matter concentration", 2021, Micromachines, 12 (4), art. no. 416, DOI: 10.3390/mi12040416

[15] J.V. Molenar, "Theoretical Analysis of PM2.5 Mass Measurements by Nephelometry", Proceedings of the Specialty Conference on PM2000: Particulate Matter and Health; Charleston, SC, USA. 24–28 January 2000.

[16] W.P. Arnott, K. Hamasha, H. Moosmüller, P.J. Sheridan, J.A. Ogren, "Towards Aerosol Light-Absorption Measurements with a 7-Wavelength Aethalometer: Evaluation with a Photoacoustic Instrument and 3- Wavelength Nephelometer". Aerosol Sci. Technol. 2005;39:17–29. doi: 10.1080/027868290901972

[17] A.D.A. Hansen, H. Rosen, T. Novakov, "The aethalometer—An instrument for the real-time measurement of optical absorption by aerosol particles". Sci. Total Environ. 1984;36:191–196. doi: 10.1016/0048-9697(84)90265-1.

[18] A. Zafra-Pérez, J. Medina-García, C. Boente, J.A. Gómez-Galán, A. Sánchez de la Campa, J.D. de la Rosa, "Designing a low-cost wireless sensor network for particulate matter monitoring: Implementation, calibration, and field-test", Atmospheric Pollution Research, Volume 15, Issue 9, 2024, 102208, ISSN 1309-1042, https://doi.org/10.1016/j.apr.2024.102208.

[19] Q. Lin, F. Zhang, W. Jiang, H. Wu, "Environmental Monitoring of Ancient Buildings Based on a Wireless Sensor Network. Sensors" 2018, 18, 4234. https://doi.org/10.3390/s18124234

[20] Z. Liu, Y. Zhang, H. Peng, "Energy balanced routing protocol based on improved particle swarm optimisation and ant colony algorithm for museum environmental monitoring of cultural relics". IET Smart Cities. 5(3), 210–219, 2023 https://doi.org/10.1049/smc2.12060

[21] A. Proietti, M. Panella, F. Leccese, E. Svezia, "Dust detection and analysis in museum environment based on pattern recognition" (2015) Measurement: Journal of the International Measurement Confederation, 66, pp. 62 - 72, . DOI: 10.1016/j.measurement.2015.01.019.

[22] T. Sharma, P. Agrawal, N. Verma, "Detection of Dust Deposition Using Convolutional Neural Network for Heritage Images", 2019, 10.1007/978-981-13-1135-2_27.

[23] H. Ben-Romdhane, D. Francis, C. Cherif, K. Pavlopoulos, H. Ghedira, S. Griffiths, "Detecting and Predicting Archaeological Sites Using Remote Sensing and Machine Learning—Application to the Saruq Al-Hadid Site", Dubai, UAE. Geosciences 2023, 13, 179. https://doi.org/10.3390/geosciences13060179

[24] T. Sharma, P. Agrawal, N. Verma, "Detection of Dust Deposition Using Convolutional Neural Network for Heritage Images". Verma, N., Ghosh, A. (eds) Computational Intelligence: Theories, Applications and Future Directions - Volume II. Advances in Intelligent Systems and Computing, 2019, vol 799. Springer, Singapore. https://doi.org/10.1007/978-981-13-1135-2_27.

[25] A. Proietti, F. Leccese, M. Caciotta, F. Morresi, U. Santamaria, C. Malomo "A new dusts sensor for cultural heritage applications based on image processing," (2014) Sensors (Switzerland), 14 (6), pp.

9813 - 9832, . DOI: 10.3390/s140609813.

[26] S.B. Lindström, R. Amjad, E. Gåhlin, L. Andersson, M. Kaarto, K. Liubytska, J. Persson, J.-E Berg, B.A. Engberg, F. Nilsson, “Pulp Particle Classification Based on Optical Fiber Analysis and Machine Learning Techniques”. Fibers 2024, 12, 2. https://doi.org/10.3390/fib12010002.

[27] Petritoli E., Leccese F., Spagnolo G.S. New reliability for industry 4.0: A caste study in COTS-based equipment (2021) 2021 IEEE International Workshop on Metrology for Industry 4.0 and IoT, MetroInd 4.0 and IoT 2021 - Proceedings, art. no. 9488555, pp. 27 - 31, . DOI: 10.1109/MetroInd4.0IoT51437.2021.9488555.

[28] Petritoli E., Leccese F. COTS Components for Space Applications: The Evaluation of Apparent Activation Energy (Eaa) (2022) 2022 IEEE 9th International Workshop on Metrology for AeroSpace, MetroAeroSpace 2022 - Proceedings, pp. 374 - 378, . DOI: 10.1109/MetroAeroSpace54187.2022.9856291.